Reaction Pathways in Solid-State Processes. 2. Carbon-13 NMR and X-ray Crystallography of Cyanobullvalene and Bullvalenecarboxylic acid

R. Poupko,[†] K. Müller,[‡] C. Krieger,[§] H. Zimmermann,[§] and Z. Luz*,[†]

Contribution from The Weizmann Institute of Science, 76100 Rehovot, Israel, Institut für Physikalische Chemie, Universität Stuttgart, D-70569 Stuttgart, Germany, and Max-Planck-Institut für Medizinische Forschung, AG Molekülkristalle, D-69120 Heidelberg, Germany

Received November 28, 1995. Revised Manuscript Received May 14, 1996[⊗]

Abstract: Carbon-13 MAS−NMR measurements and the X-ray crystallographic structure of cyanobullvalene (I) and bullvalenecarboxylic acid (II) are reported. The two compounds crystallize as isomer 3 in the triclinic space group $P\bar{1}$. Two-dimensional solid-state NMR exchange experiments indicate the occurrence of bond shift (Cope) rearrangement in both cases. Analysis of the results shows that the process involves isomer 1 as a transient intermediate. The Arrhenius kinetic parameters were determined from the line broadening in the 1D MAS spectra and magnetization transfer experiments as function of temperature, yielding, $A_C = 1.0 \times 10^{12}$ s^{-1}, 2.2×10^{12} s^{-1} and $E_C = 13.9$ kcal mol^{-1}, 14.1 kcal mol^{-1} for compounds I and II, respectively. A rearrangement process involving isomer 2 as an intermediate may also occur, but it does not result in permutation of atoms and therefore is NMR-invisible. NMR exchange measurements on solid cyclooctatetraene dimer (III) were also carried out; however, on the time scale of up to 1 min no dynamic effects are observed.

Introduction

In two previous papers in this series we presented dynamic NMR studies in solutions of fluorobullvalene, cyanobullvalene, and bullvalenecarboxylic acid[1] as well as in solid fluorobullvalene.[2] All compounds exhibit fast Cope rearrangement in solution at rates comparable to those for the unsubstituted bullvalene.[3,4] However, while for unsubstituted bullvalene the rate of the Cope rearrangement in the solid state is essentially the same as in solution,[5,6] the corresponding rates in solid fluorobullvalene were found to be considerably slower than in solution. This difference was explained[2] in terms of the different stabilities of the intermediate isomers in the two systems. While for unsubstituted bullvalene a single rearrangement step is always permissible, in substituted bullvalenes, single rearrangements may lead to isomers that are not easily accommodated in the crystal lattice, thus slowing down, or even completely hindering, the reaction.

In the present paper we extend the study of the Cope rearrangement in solid substituted bullvalenes to cyanobullvalene (I) and bullvalenecarboxylic acid (II). From X-ray measurements we find that these compounds crystallize as isomer 3, i.e., with the substitution at carbon 3, next to the bridgehead carbon. For comparison we have also studied the homotropylidene derivative, cyclooctatetraene (COT) dimer (III), which

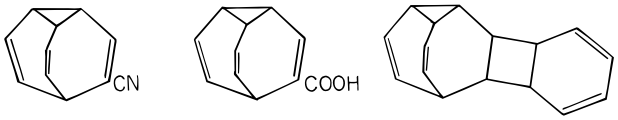

in solution is known to undergo rapid bond shift rearrangement.[7] In these compounds the C_3 symmetry of the bullvalene core is removed, and, therefore, in ordered crystals, 3-fold jumps as occur in bullvalene and in fluorobullvalene (which crystallizes as isomer 4 with the fluorine bound to the bridgehead carbon) are not allowed. Cope rearrangement in the monosubstituted bullbalenes can in principle still take place, however, only via short lived transient intermediates, as found for fluorobullvalene.[2] We find that indeed, within our experimental sensitivity, no reorientation jumps take place in these compounds. However, while compounds I and II undergo Cope rearrangement, no such process takes place in compound III. Using 2D exchange spectrocopy we are able to uniquely identify the pathway of the reaction in compounds I and II, and from the line broadening in the 1D MAS spectra and magnetization transfer experiments we determine the rates of the reaction.

Crystal Structure

In this section we report the crystal structure of cyanobullvalene (I) and bullvalenecarboxylic acid (II) as determined by X-ray diffractometry. No measurements were made on compound III. The structure of I was reported in the Ph.D. dissertation of T. Zwez,[8] but the results were incomplete. The experimental details are as in the preceding paper.[2]

Both compounds I and II crystallize entirely in the form of isomer 3, in the triclinic space group $P\bar{1}$ (no. 2 in the International Crystallographic Tables). The lattice parameters are $a = 8.913(2)$Å, $b = 9.555(1)$Å, $c = 10.234(2)$Å, $\alpha = 78.36(1)°$, $\beta = 89.01(2)°$, $\gamma = 74.77(1)°$ for I and $a = 7.162(2)$Å, b

[†] The Weizmann Institute of Science.
[‡] Universität Stuttgart.
[§] Max-Planck-Institut für Medizinische Forschung.
[⊗] Abstract published in *Advance ACS Abstracts,* August 1, 1996.

(1) Poupko, R.; Zimmermann, H.; Müller, K.; Luz, Z. *J. Am. Chem. Soc.* **1996**, *118*, 7995.
(2) Müller, K.; Zimmermann, H.; Krieger, C.; Poupko, R.; Luz, Z. *J. Am. Chem. Soc.* **1996**, *118*, 8006.
(3) Oth, J. F. M.; Müller, K.; Gilles, J.-M.; Schröder, G. *Helv. Chim. Acta* **1974**, *57*, 1415.
(4) Poupko, R.; Zimmermann, H.; Luz, Z. *J. Am. Chem. Soc.* **1984**, *106*, 5391.
(5) Schlick, S.; Luz, Z.; Poupko, R.; Zimmermann, H. *J. Am. Chem. Soc.* **1992**, *114*, 4315.
(6) Luz, Z.; Poupko, R.; Alexander, S. *J. Chem. Phys.* **1993**, *99*, 7544.
(7) Nakanishi, H.; Yamamoto, O. *Chem. Lett.* **1973**, p 1273.
(8) Zwez, T. Ph.D. Dissertation, Karlsruhe University, 1988.

S0002-7863(95)04006-6 CCC: $12.00

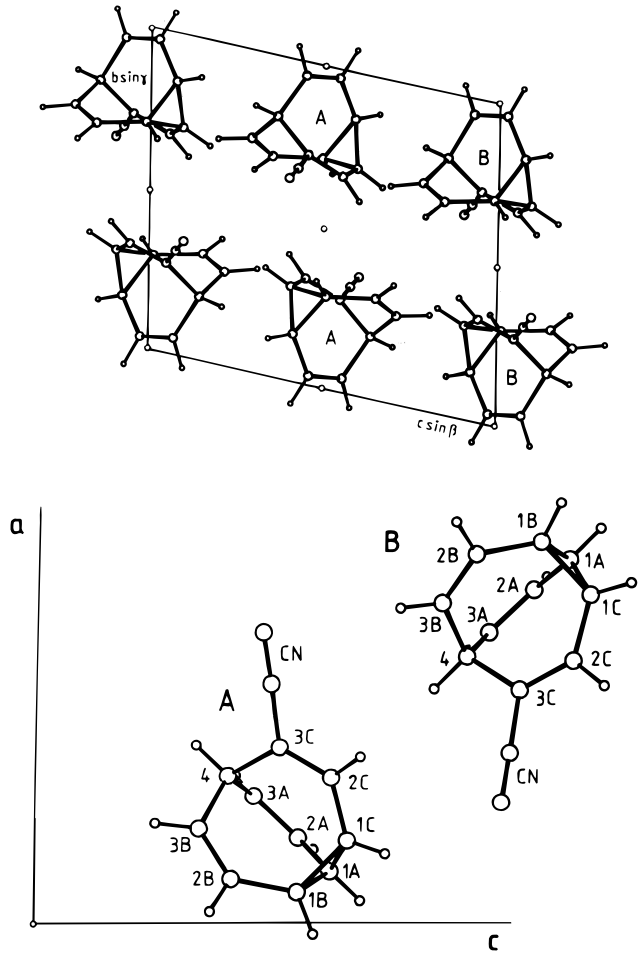

Figure 1. Top: Projections of the crystal structure of cyanobullvalene down the *a* axis. Bottom: Projection of two inequivalent molecules in the crystal down the *b** axis and the labeling system used.

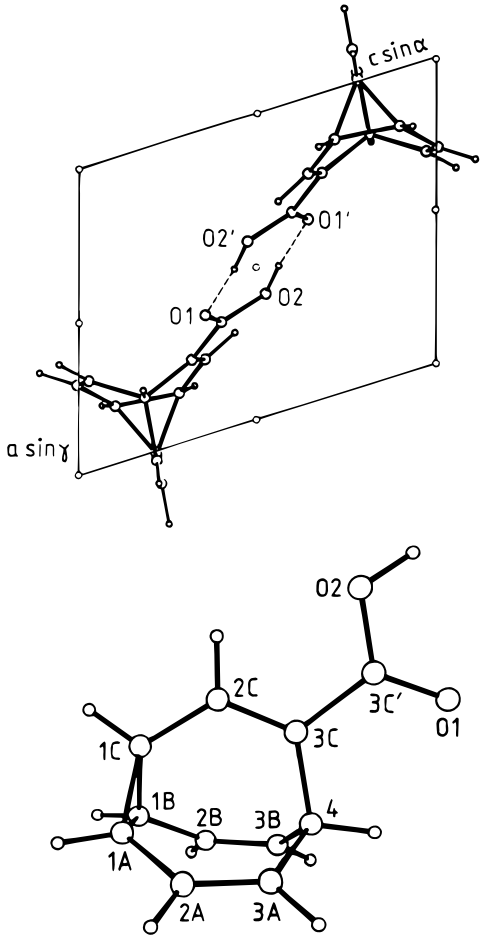

Figure 2. Top: Projection of the bullvalene carboxylic acid dimer down the *b** axis. Bottom: A perspective view of the bullvalene carboxylic acid molecule and the labeling system used.

$= 7.261(1)$Å, $c = 8.871(2)$Å, $\alpha = 80.56(2)°$, $\beta = 71.96(2)°$, $\gamma = 84.62(2)°$ for II. In this connection it is worth mentioning that ethylthiobullvalene also crystallizes as isomer 3 but in a different crystallographic space group, $I\bar{4}$.[9]

In cyanobullvalene there are four molecules per unit cell, two pairs related to each other by an inversion center. Within each pair the molecules are not symmetry related and therefore have slightly different geometries. Projections of the crystal structure down the *a* axis and of the two types of inequivalent molecules down the *b** axis are shown in Figure 1. The bullvalene cage in both molecules is nearly 3-fold symmetric with angles between the wings (respectively opposite wings A, B, and C) of 118.1°, 120.7°, and 121.2° for molecule A and 117.5°, 120.9°, and 121.6° for molecule B.

In bullvalenecarboxylic acid there are two centrosymmetric hydrogen bonded molecules per unit cell as shown in Figure 2. The molecules have nearly C_s symmetry with the reflection plane including the C-wing carbons and the carboxylic acid group. The plane of the carboxy group is slightly (∼8°) rotated away from that of wing C. The bullvalene cage is however nearly 3-fold symmetric with interwing angles of 118.6°, 120.6°, and 120.8°, opposite wings A, B, and C, respectively. Crystallographic coordinates for the non-hydrogen atoms in compounds I and II are given in Tables 1 and 2, respectively. The complete data and the parameters of the structure refinements have been deposited with the Cambridge Crystallographic Data Center, 12 Union Road, Cambridge CB2 1EZ, United Kingdom.

(9) Luger, P.; Roth, K. *J. Chem. Soc., Perkin Trans. II* **1989**, 649.

Carbon-13 NMR in the Solid State

A. Cyanobullvalene (I). Carbon-13 CPMAS spectra of cyanobullvalene at different temperatures are depicted in Figure 3. For the experimental details we refer to the preceding paper.[2] The spectra are fully consistent with isomer 3 being the sole species in the crystal as may be judged by comparing the chemical shifts of the center bands with the solution spectrum of cyanobullvalene.[1] The peak assignment is given in the bottom trace of the figure. The intensity of the various peaks are not always stoichiometric (see in particular the CN signal) due to differences in the cross polarization efficiencies. It may be noticed that some of the carbons, in particular those associated with the substituted wing (wing C), exhibit a sharp doublet. This reflects the fact that there are two types of inequivalent molecules in the unit cell (Figure 1). Some structure is also observed in other signals as for example in that of carbons 1A and 1B (labeled as 1AB), but for some reason, the effect is more pronounced in the signals associated with the carbons in wing C. We shall disregard this fine structure in the discussion that follows (although we include it in the line shape simulation). From such CPMAS spectra, recorded at room temperature for several different spinning frequencies, we have derived values for the chemical shift tensors of the various carbons.[10] The results are summarized in Table 3.

Figure 3 also shows the temperature dependence of the spectra up to almost the melting point (57 °C). There is clearly a

(10) Herzfeld, J.; Berger, A. E. *J. Chem. Phys.* **1980**, *73*, 6021.

Table 1. Atomic Coordinates and Isotropic Displacement Parameters of Non-Hydrogen Atoms in Cyanobullvalene[a]

	molecule A				molecule B			
atom	*x*	*y*	*z*	$U_{eq}\cdot\frac{10^4}{Å^2}$	*x*	*y*	*z*	$U_{eq}\cdot\frac{10^4}{Å^2}$
4	0.3004(2)	0.1915(2)	0.3630(2)	467(4)	0.5863(2)	0.1994(2)	0.8548(2)	516(4)
3C	0.3433(2)	0.2861(2)	0.4517(1)	395(3)	0.4827(2)	0.2822(2)	0.9508(2)	417(3)
2C	0.2576(2)	0.3992(2)	0.5519(2)	443(4)	0.5399(2)	0.3196(2)	1.0546(1)	432(3)
1C	0.1128(2)	0.2943(2)	0.5940(2)	512(4)	0.7032(2)	0.2904(2)	1.0932(2)	505(4)
3A	0.2916(2)	0.0437(2)	0.4443(2)	557(4)	0.6818(2)	0.0515(2)	0.9272(2)	605(4)
2A	0.1939(2)	0.0286(2)	0.5407(2)	592(5)	0.7866(2)	0.0341(2)	1.0226(2)	628(5)
1A	0.0798(2)	0.1470(2)	0.5864(2)	544(4)	0.8257(2)	0.1515(2)	1.0745(2)	580(4)
3B	0.1477(2)	0.2742(2)	0.2894(2)	557(4)	0.6833(2)	0.2941(2)	0.7839(2)	606(5)
2B	0.0155(2)	0.3143(2)	0.3499(2)	561(4)	0.7875(2)	0.3365(2)	0.8457(2)	601(4)
1B	−0.0084(2)	0.2866(2)	0.4930(2)	532(4)	0.8272(2)	0.2992(2)	0.9879(2)	551(4)
C	0.4821(2)	0.3340(2)	0.4231(2)	432(4)	0.3182(2)	0.3272(2)	0.9245(2)	458(4)
N	0.5936(1)	0.3701(2)	0.3982(2)	594(4)	0.1871(2)	0.3629(2)	0.9019(2)	634(4)

[a] $U_{eq} = \frac{1}{3}\sum\sum U_{ij}\mathbf{a}_i\cdot\mathbf{a}_j a_i^* a_j^*$.

Table 2. Atomic Coordinates of the Non-Hydrogen Atoms in Bullvalenecarboxylic Acid[a]

atom	*x*	*y*	*z*	$U_{eq}\cdot\frac{10^4}{Å^2}$
1A	−0.0103(3)	0.0134(3)	0.2210(2)	620(5)
1B	0.1901(3)	−0.0122(3)	0.1031(2)	582(5)
1C	0.1667(3)	−0.0446(3)	0.2838(2)	574(5)
2A	−0.1119(3)	0.1947(3)	0.2354(2)	653(6)
2B	0.2975(3)	0.1433(3)	−0.0040(2)	601(5)
2C	0.2493(2)	0.0798(2)	0.3569(2)	466(4)
3A	−0.0314(3)	0.3556(3)	0.2220(2)	668(5)
3B	0.2993(3)	0.3139(3)	0.0288(2)	581(5)
3C	0.2614(2)	0.2648(2)	0.3192(2)	451(4)
4	0.1870(3)	0.3762(3)	0.1865(2)	555(5)
3C′	0.3581(2)	0.3671(2)	0.4018(2)	443(4)
O(1)	0.3973(2)	0.5319(2)	0.3570(1)	616(3)
O(2)	0.4055(2)	0.2707(2)	0.5253(1)	587(3)

[a] $U_{eq} = \frac{1}{3}\sum\sum U_{ij}\ \mathbf{a}_i\cdot\mathbf{a}_j a_i^* a_j^*$.

Table 3. The Chemical Shift Tensor Components (in ppm) of the Various Carbons in Compounds I and II[a]

	I				II			
	δ_{iso}[c]	δ_{xx}	δ_{yy}	δ_{zz}	δ_{iso}	δ_{xx}	δ_{yy}	δ_{zz}
1C	21.8 22.6	34	0	−34	22.7	29	6	−35
2C	146.0 147.1	106	−20	−86	146.1	105	−14	−91
3C	110.3 111.8	80	0	−80	126.8	85	−12	−73
4	34.0				28.8	10	0	−10
1AB	24.3	34	0	−34	24.4[d] 25.8[d]	28	5	−33
2AB	130.0	93	0	−93	128.8	89	6	−95
3AB	125.7	98	−10	−88	127.7	89	6	−95
X[b]	119.7 122.6	200	−100	−100	172.7	64	0	−64

[a] The isotropic chemical shifts are relative to TMS (estimated accuracy ±0.2 ppm). The principal components of the anisotropic part are relative to the corresponding δ_{iso}, so that $\delta_{xx} + \delta_{yy} + \delta_{zz} = 0$ (estimated accuracy ±6 ppm). [b] X corresponds to the CN and COOH carbons in compounds I and II, respectively. [c] The two entries in this column correspond to the two inequivalent molecules in the unit cell. [d] The two entries for the 1AB carbons of compound II reflect the small inequivalence of 1A and 1B.

selective line broadening effect, whereby all peaks, except those associated with the carbons in wing C, undergo broadening, while the latter remain sharp. Such an effect cannot be due to reorientation, since this would result in a similar line broadening of corresponding atoms in all wings. We therefore conclude that the effect is due to permutation of carbon atoms by a very specific Cope rearrangement. As in the case of fluorobullvalene,[2] since the crystal consists of a single isomer the process must proceed via transient intermediates in a way that restores the ground-state isomer 3 to its original position in the crystal lattice.

To discuss the possible mechanisms that might be responsible for the line broadening in the 1D spectra it is convenient to apply 2D exchange spectroscopy.[11] We use again the rotor synchronized 2D exchange MAS experiment[12,13] described in the previous paper.[2] One such spectrum is shown in Figure 4. It was recorded at 30 °C with a mixing time of 30 ms and a recycle time of 13.6 min. (The T_1 of the carbons is approximately 100 min at room temperature.) The spectrum exhibits clear hetero cross peaks interlinking the signals of carbons 1AB, 2AB, 3AB, and 4, while the signals of the substituted wing C carbons (1C, 2C, 3C, and CN) show no cross peaks at all. This result is completely consistent with the behavior of the 1D spectra (Figure 3) and confirms the occurrence of a Cope rearrangement in solid cyanobullvalene. Spin diffusion can be ruled out on the basis of the time scale involved (30 ms), the strong temperature dependence of the line broadening, and in particular the selective cross peak pattern (or broadening) found experimentally.

Following the discussion for fluorobullvalene[2] and the general interconversion scheme between the monosubstituted bullvalene isomers,[1] the following reaction pathways must be considered

$$\text{(i)}\ 3 \xrightarrow{a} 2 \xrightarrow{a} 3$$

$$\text{(ii)}\ 3 \xrightarrow{a} 2 \xrightarrow{s} 2 \xrightarrow{a} 3$$

$$\text{(iii)}\ 3 \xrightarrow{a} 2 \xrightarrow{s} 2 \xrightarrow{s} 2 \xrightarrow{a} 3$$

$$\text{(iv)}\ 3 \xrightarrow{s} 1 \xrightarrow{s} 3$$

$$\text{(v)}\ 3 \xrightarrow{s} 1 \xrightarrow{a} 4 \rightarrow 1 \xrightarrow{s} 3$$

where the letters *a* and *s* indicate whether a bond opposite the

(11) Ernst, R. R.; Bodenhausen, G.; Wokaun, A. Principles of Nuclear Magnetic Resonance in One and Two Dimensions; Clarendon Press: Oxford, 1987; Chapter 9.

(12) Kentgens, A. P. M.; de Jong, A. F.; de Boer, E.; Veeman, W. S. *Macromolecules* **1985**, *18*, 1045. Kentgens, A. P. M.; de Boer, E.; Veeman, W. S. *J. Chem. Phys.* **1987**, *87*, 6859.

(13) Hagemeyer, A.; Schmidt-Rohr, K.; Spiess, H. W. *Adv. Magn. Reson.* **1989**, *13*, 85.

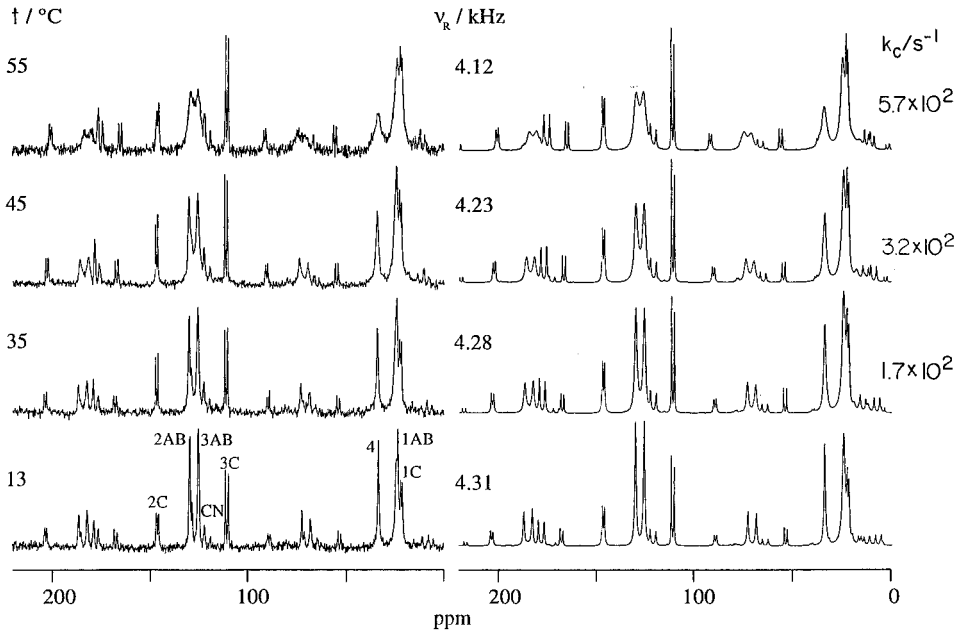

Figure 3. Left: CPMAS ^{13}C NMR spectra of cyanobullvalene at different temperatures as indicated. Spinning rate varied between 4.1 and 4.3 kHz, recycle time 10 min, number of scans between 30 and 60. Right: Simulated dynamic MAS spectra calculated as described in the text.

substituted wing is cleaved (*a*) or next to it (*s*). The pathway that actually occurs in nature may be identified by comparing the experimental 2D exchange spectrum with the patterns predicted by the various mechanisms. The first mechanism (i) involves isomer 2 as the only transient intermediate

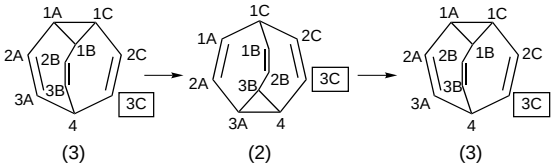

In the notation of the numerical diagrams described in the preceding paper[2] this reaction may be written as follows

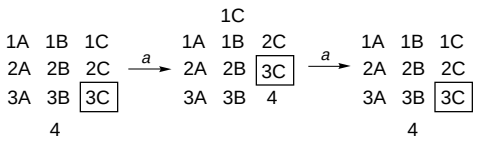

where the substituted atoms are enclosed in squares. Since, however, the interconversion between isomers 3 and 2 involves cleavage and reforming of the same (*a*) bond (the column of the C-wing atoms that is "pushed up" in the first stage is also "pushed down" in the second stage), the process does not lead to any permutation of atoms and will therefore not affect the NMR spectrum. Thus, although this process may well occur in solid cyanobullvalene it will not be detected by NMR.

There are two equivalent sequences corresponding to mechanism (ii); one of them is

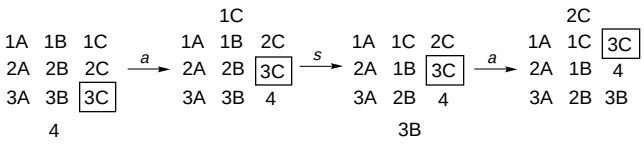

Note that since the number of steps in the above sequence is odd, an inverted molecule is obtained, with the bridgehead atom at the top and the cyclopropane ring at the bottom. To revert the molecule to its original orientation the molecules undergo an extra π-flip about an axis perpendicular to the pseudo C_3 axis of the bullvalene cage resulting in the end diagram

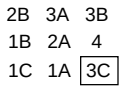

In the alternative sequence, instead of wing B, wing A is pushed down in the second step, resulting in the end diagram

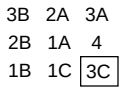

Assuming that both cycles are equally probable the following overall permutation matrix, $P_{33}^{2,2}$, is obtained

$P_{33}^{2,2}$ =

	1A	1B	1C	2A	2B	2C	3A	3B	3C	4
1A	-1				$\frac{1}{2}$			$\frac{1}{2}$		
1B		-1		$\frac{1}{2}$			$\frac{1}{2}$			
1C			-1				$\frac{1}{2}$	$\frac{1}{2}$		
2A		$\frac{1}{2}$		-1	$\frac{1}{2}$					
2B	$\frac{1}{2}$			$\frac{1}{2}$	-1					
2C						-1				1
3A		$\frac{1}{2}$	$\frac{1}{2}$				-1			
3B	$\frac{1}{2}$		$\frac{1}{2}$					-1		
3C									0	
4						1				-1

where the superscripts refer to the intermediates involved in the reaction and the subscripts to the initial and final isomers. The corresponding exchange matrix is $K_{33}^{2,2} = k_{33}^{2,2}P_{33}^{2,2}$, where $k_{33}^{2,2}$ is the rate constant associated with this mechanism. For the calculation of the dynamic MAS spectra, to be described shortly, the full exchange matrix need to be used, but for the discussion of the 2D exchange results in terms of the various

mechanisms it is sufficient to consider the effect on the center bands (the isotropic spectrum) only. The pairs of atoms (1A, 1B), (2A, 2B), and (3A, 3B) then become equivalent (and are labeled, respectively, 1AB, 2AB, 3AB) and the contracted exchange matrix becomes

	1AB	2AB	3AB	4	1C	2C	3C
1A	-1	$\frac{1}{2}$	$\frac{1}{2}$				
2AB	$\frac{1}{2}$	$-\frac{1}{2}$					
3AB	$\frac{1}{2}$		-1		1		
4				-1		1	
1C			$\frac{1}{2}$		-1		
2C				1		-1	
3C							0

where we have rearranged the order of the columns (and rows) to facilitate comparison with other mechanisms. Note that atom 3C must remain invariant by the basic assumption that the crystal order is maintained (assuming, of course, that there is no cleavage of the 3C-CN bond). The same argument applies to the CN carbon, which has been left out from the diagrams altogether.

Mechanism (iii) may be represented by the sequence

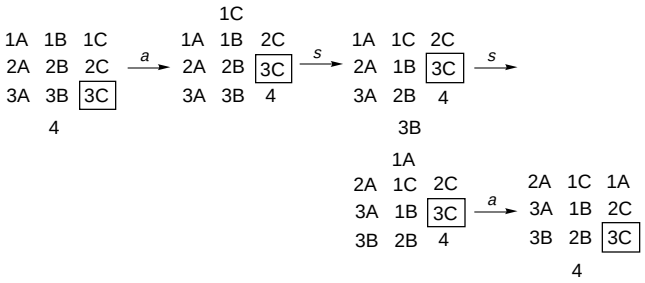

and an equivalent sequence in which wings A and B are interchanged in the second and third steps, leading to the end diagram

1C 2B 1B
1A 3B 2C
2A 3A 3C
4

The overall permutation matrix, $P_{33}^{2,2,2}$, then becomes

	1A	1B	1C	2A	2B	2C	3A	3B	3C	4
1A	-1		$\frac{1}{2}$	$\frac{1}{2}$						
1B		-1	$\frac{1}{2}$		$\frac{1}{2}$					
1C	$\frac{1}{2}$	$\frac{1}{2}$	-1							
2A	$\frac{1}{2}$			-1			$\frac{1}{2}$			
2B		$\frac{1}{2}$			-1			$\frac{1}{2}$		
2C						0				
3A				$\frac{1}{2}$			-1	$\frac{1}{2}$		
3B					$\frac{1}{2}$		$\frac{1}{2}$	-1		
3C									0	
4										0

which as above can be contracted to

	1AB	2AB	3AB	4	1C	2C	3C
1AB	-1	$\frac{1}{2}$			1		
2AB	$\frac{1}{2}$	-1	$\frac{1}{2}$				
3AB		$\frac{1}{2}$	$-\frac{1}{2}$				
4				0			
1C	$\frac{1}{2}$				-1		
2C						0	
3C							0

Mechanism (iv), which involves isomer 1 as an intermediate, can be written as follows

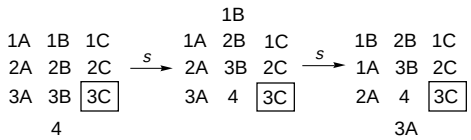

with an equivalent pathway leading to

2A 1A 1C
3A 1B 2C
4 2B 3C
3B

Both pathways correspond to simple seven cycle permutations involving carbon 4 and those of wings A and B. The full and contracted permutation matrices, P_{33}^{1}, then become

	1A	1B	1C	2A	2B	2C	3A	3B	3C	4
1A	-1	$\frac{1}{2}$		$\frac{1}{2}$						
1B	$\frac{1}{2}$	-1			$\frac{1}{2}$					
1C			0							
2A	$\frac{1}{2}$			-1			$\frac{1}{2}$			
2B		$\frac{1}{2}$			-1			$\frac{1}{2}$		
2C						0				
3A				$\frac{1}{2}$			-1			$\frac{1}{2}$
3B					$\frac{1}{2}$			-1		$\frac{1}{2}$
3C									0	
4							$\frac{1}{2}$	$\frac{1}{2}$		-1

and

	1AB	2AB	3AB	4	1C	2C	3C
1AB	$-\frac{1}{2}$	$\frac{1}{2}$					
2AB	$\frac{1}{2}$	-1	$\frac{1}{2}$				
3AB		$\frac{1}{2}$	-1	1			
4			$\frac{1}{2}$	-1			
1C					0		
2C						0	
3C							0

For sequence (v) the statistics are slightly more involved, because each of the two 3 → 1 branches, bifurcate twice at, respectively, the 4 → 1 and 1 → 3 interconversions. We show in Scheme 1 half of the branching scheme, starting with isomer 1 of the previous scheme. Note that in the last step (1 → 3) we

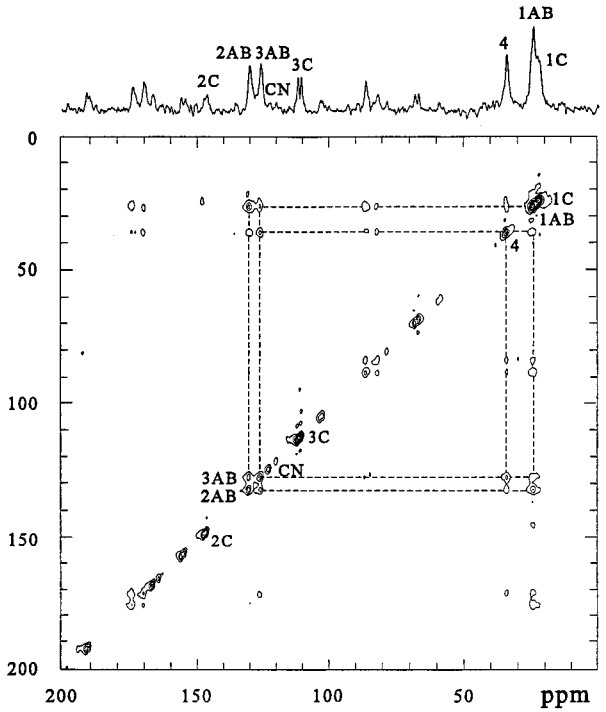

Figure 4. A rotor synchronized carbon-13 MAS 2D exchange spectrum of cyanobullvalene at 30 °C with spinning frequency 3.3 kHz and a mixing time $\tau_m = 30$ ms. Sixty-four t_1 increment of 50 μs were recorded with eight-phase cycled scans per t_1 point. The dwell time was 50 μs yielding a sweep width of 20 kHz in both dimensions. The recycle time was 13.6 min resulting in a total recording time of 4.8 days. Ten equidistant contours are plotted.

added a 3-fold rotation to bring atom 3C back to its original site in the diagram. The full and contracted permutation matrices, $P_{33}^{1,4,1}$, are

	1A	1B	1C	2A	2B	2C	3A	3B	3C	4
1A	$-\frac{6}{8}$	$\frac{3}{8}$		$\frac{1}{8}$	$\frac{2}{8}$					
1B	$\frac{3}{8}$	$-\frac{6}{8}$		$\frac{2}{8}$	$\frac{1}{8}$					
1C			-1	$\frac{2}{8}$	$\frac{2}{8}$		$\frac{2}{8}$	$\frac{2}{8}$		
2A	$\frac{1}{8}$	$\frac{2}{8}$	$\frac{2}{8}$	-1	$\frac{2}{8}$			$\frac{1}{8}$		
2B	$\frac{2}{8}$	$\frac{1}{8}$	$\frac{2}{8}$	$\frac{2}{8}$	-1		$\frac{1}{8}$			
2C						-1	$\frac{2}{8}$	$\frac{2}{8}$		$\frac{4}{8}$
3A			$\frac{2}{8}$		$\frac{1}{8}$	$\frac{2}{8}$	-1	$\frac{2}{8}$		$\frac{1}{8}$
3B			$\frac{2}{8}$	$\frac{1}{8}$		$\frac{2}{8}$	$\frac{2}{8}$	-1		$\frac{1}{8}$
3C									0	
4						$\frac{4}{8}$	$\frac{1}{8}$	$\frac{1}{8}$		$-\frac{6}{8}$

and

	1AB	2AB	3AB	4	1C	2C	3C
1AB	$-\frac{3}{8}$	$\frac{3}{8}$					
2AB	$\frac{3}{8}$	$-\frac{6}{8}$	$\frac{1}{8}$		$\frac{4}{8}$		
3AB		$\frac{1}{8}$	$-\frac{6}{8}$	$\frac{2}{8}$	$\frac{4}{8}$	$\frac{4}{8}$	
4			$\frac{1}{8}$	$-\frac{6}{8}$		$\frac{4}{8}$	
1C		$\frac{2}{8}$	$\frac{2}{8}$		-1		
2C			$\frac{2}{8}$	$\frac{4}{8}$		-1	
3C							0

Scheme 1

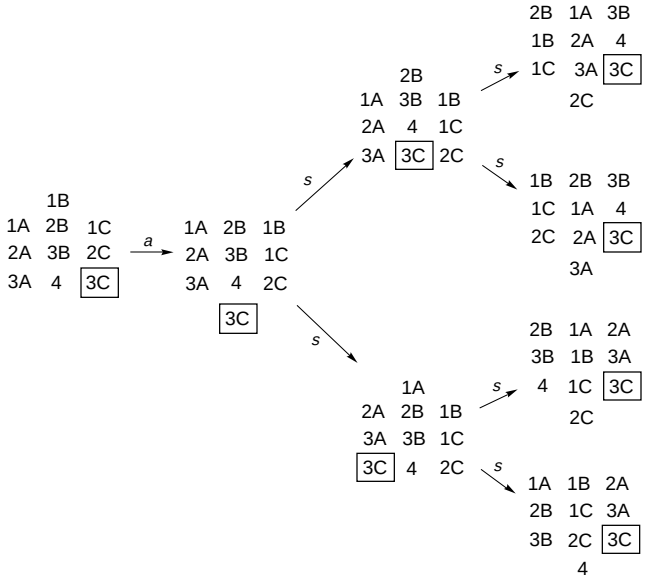

With these results we can now identify the rearrangement pathway that actually occurs in solid cyanobullvalene. We recall that in the experimental 2D exchange spectrum (Figure 4) all atoms of wing C remain invariant, i.e., do not show any cross peaks. Referring to the permutation matrices of mechanisms (ii)−(v) (remembering that mechanism (i) does not result in permutation of atoms) we note that only mechanism (iv) is consistent with this observation, i.e., permutation of all atoms in wings A and B and atom 4, leaving atoms 1C, 2C, and 3C (and CN) invariant. All other mechanisms are inconsistent with the experimental 2D spectrum.

In principle we could estimate the rate constant for this reaction, k_{33}^1, by a quantitative analysis of the cross peak intensities in 2D exchange spectra recorded as a function of τ_m. However such experiments are too time consuming, and the results can more readily be obtained from magnetization transfer experiments or from the line broadening in 1D spectra (see below). Inspection of the 2D spectrum in Figure 4 shows, however, that it corresponds to $k_{33}^1 \lesssim \tau_m^{-1}$. This follows from the following argument: According to the contracted permutation matrix for mechanism (iv), first order cross peaks (linear in τ_m) are expected between the pairs (1AB, 2AB), (2AB, 3AB), and (3AB, 4) and only second order cross peaks (which initially increase quadratically with τ_m) for the pairs (1AB, 3AB) and (2AB, 4), while the cross peaks (1AB, 4) are of third order (and should have a cubic dependence on the mixing time). Referring to Figure 4 we note that indeed the first order cross peaks are the strongest, while the third order cross peaks (despite the fact that they link between the strongest diagonal peaks) are the weakest ones in the spectrum. Thus at 30 °C, $k_{33}^1 \lesssim 30\ s^{-1}$.

We now use the 1D spectra of the type shown in Figure 3 for a quantitative determination of k_{33}^1 at different temperatures. For room temperature and below, where the line broadening is small, we applied magnetization transfer experiments of the type discussed by Szeverenyi et al.[14] for tropolone, using the full exchange matrix in the analysis. When the dynamic line broadening was significant (above room temperature) we made a complete line shape analysis using the Floquet method[15,16] as described in ref 2. For the latter calculations

(14) Szeverenyi, N. M.; Bax, A.; Maciel, G. E. *J. Am. Chem. Soc.* **1983**, *105*, 2579.
(15) Schmidt, A.; Vega, S. *J. Chem. Phys.* **1987**, *87*, 6895.
(16) Luz, Z.; Poupko, R.; Alexander, S. *J. Chem. Phys.* **1993**, *99*, 7544.

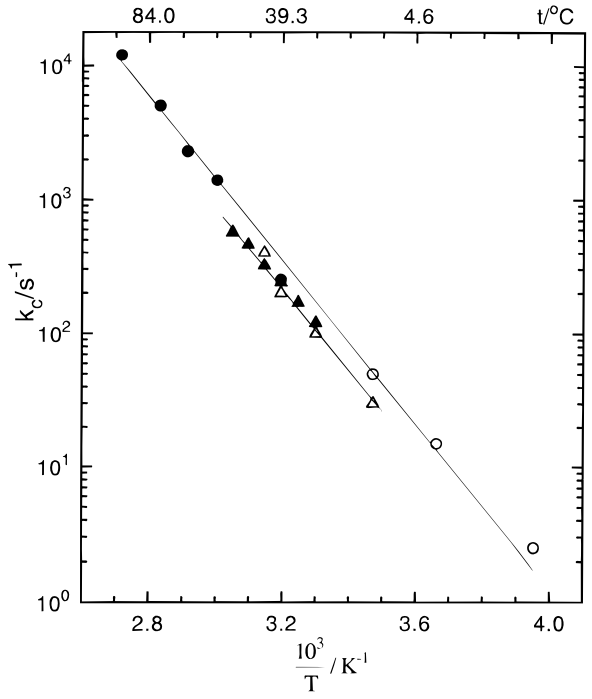

Figure 5. Arrhenius plots for k^1_{33} in cyanobullvalene (triangles) and bullvalenecarboxylic acid (circles). The results indicated by fill symbols were obtained from the line shape fitting. Those indicated by open symbols were obtained from magnetization transfer.

we made the same assumption concerning the orientations of the chemical shift tensors as for fluorobullvalene, using the magnetic parameters from Table 3, with the full exchange matrix K^1_{33}. Since the exchanging carbons do not show well resolved peaks for the two crystallographically inequivalent sites, as do the invariant carbons, we assumed a single rate constant for both. Examples of simulated spectra are shown in the right column of Figure 3. In these simulations the overall intensity of carbons CN, 2C, and 3C are normalized to 0.65 and that of the 1C carbon to 0.52, while all others were taken as 1. The exchange invariant $1/T_2^\circ$ was 380 s^{-1} for the 1AB peak (to account for the structural features), 70 s^{-1} for the two 3C peaks, and 140 s^{-1} for all other peaks.

The results obtained for k^1_{33} by both methods are plotted versus the reciprocal absolute temperature in Figure 5, yielding an Arrhenius equation with a pre-exponential parameter $A_C = 1.0 \times 10^{12}$ s^{-1} and an activation energy $E_C = 13.9$ kcal mol^{-1}.

Before concluding the cyanobullvalene section we wish to indicate that in a 2D exchange experiment performed with a much longer (700 ms) mixing time than used in Figure 4, weak additional cross peaks were detected (for example between carbons 1C and 2C). The quality of this spectrum was not sufficient to draw definite conclusions, but it might indicate the onset of additional rearrangement mechanisms at a longer time scale.

B. Bullvalenecarboxylic Acid (II). The situation in bullvalenecarboxylic acid is very similar to that in cyanobullvalene. It crystallizes as isomer 3, with two centrosymmetric molecules in the unit cell. The molecules have nearly C_s symmetry with wing C serving as a pseudo mirror plane. Consequently almost no structural splittings are observed in the ^{13}C MAS spectrum of this compound. The only exception is the 1AB signal which exhibits a small splitting due to a slight inequivalence of the 1A and 1B carbons (see the −20 °C spectrum in Figure 6). The isotropic chemical shifts are very similar to those found for isomer 3 in solution. The principal values of the chemical shift tensors for the various carbons derived from the side band intensities in MAS spectra are summarized in Table 3.

On heating line broadening sets in with similar selectivity as found for cyanobullvalene. The carboxyl and wing C carbons remain sharp, while all other peaks including that of carbon 4 broaden. Similarly, a 2D exchange spectrum (Figure 7), recorded under very similar conditions as those used for recording the 2D spectrum of cyanobullvalene, exhibits essentially the same features as in the latter. In particular there are hetero cross peaks linking the signals of carbons 1AB, 2AB, 3AB, and 4, but none involving the carbons of the substituted wing C.

The discussion of the results for cyanobullvalene is thus also applicable to bullvalenecarboxylic acid and will therefore not be repeated. In the right column of Figure 6 are shown simulated spectra that fit the corresponding experimental ones. The rate constants derived from such fittings and from magnetization transfer experiments are plotted, together with those for cyanobullvalene, in Figure 5. They correspond to an Arrhenius law with $A_C = 2.2 \times 10^{12}$ s^{-1} and $E_C = 14.1$ kcal mol^{-1}.

C. Cyclooctatetraene (COT) Dimer (III). The degenerate Cope rearrangement in solutions of the COT dimer was studied by Nakanishi and Yamamoto[7] using carbon-13. The reaction is very fast and at room temperature has a rate constant of almost 10^6 s^{-1}. To check whether the reaction also occurs in solid COT dimer, carbon-13 1D- and 2D-exchange spectra were recorded over a wide range of temperatures and mixing times. In Figure 8 are shown carbon-13 spectra of solid COT dimer using CPMAS at room temperature and of COT dimer dissolved in CD_2Cl_2 at −73 °C where the rearrangement rate is slow. The peak assignment for the solution spectrum is indicated in the figure. It is based on a detailed analysis of the proton spectrum (COSY and 2D-exchange at 200 K), $^1H-^{13}C$ correlation, and carbon-13 2D-exchange. This assignment differs in several details from that given in ref 7.

Unlike in the previous two compounds, the carbon-13 MAS spectrum of III does not exhibit any dynamic effects. There is no line broadening and no magnetization transfer effects in 1D spectra on heating up to 65 °C nor are there any cross peaks in 2D exchange spectra with mixing times of up to 20 s at 55 °C. This indicates that on this time scale no rearrangement takes place and suggests that the crystal is well ordered with the orientation of the bridgehead carbon and the cyclopropane ring well defined in the lattice. An interconversion (first step in the diagram below)

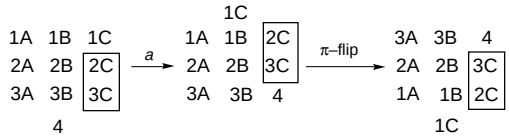

may cause crystal disorder, even if coupled with a π-flip (second step in the diagram). Apparently the lattice packing forces are too strong to allow such a process to occur.

Summary and Conclusions

We have shown that cyanobullvalene and bullvalenecarboxylic acid crystallize as well ordered lattices with isomer 3 as the sole species in the lattice. Because these molecules lack 3-fold symmetry no 3-fold jumps can take place, as was found to be the case for unsubstituted bullvalene or in fluorobullvalene (isomer 4) in the solid state. Both molecules undergo however bond shift rearrangement in the solid state, and it was shown that the process involves isomer 1 as a transient intermediate.

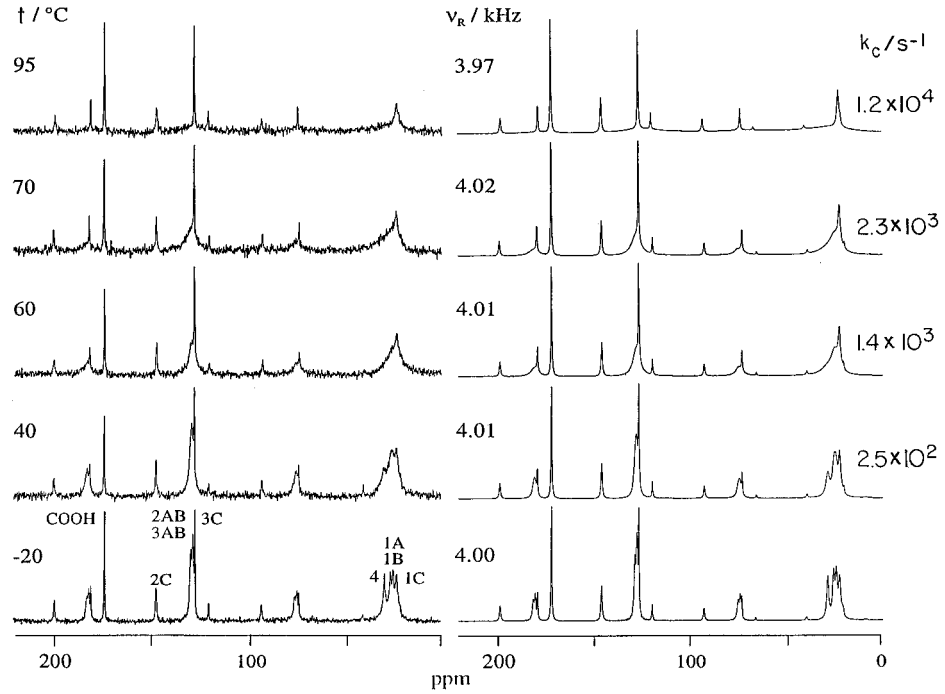

Figure 6. Left: CPMAS ^{13}C spectra of bullvalenecarboxylic acid at different temperatures as indicated. Spinning rate $\nu_R \simeq 4.0$ kHz, recycle time 10 min, number of scans per spectrum 12 to 60. Right: Simulated dynamic MAS spectra.

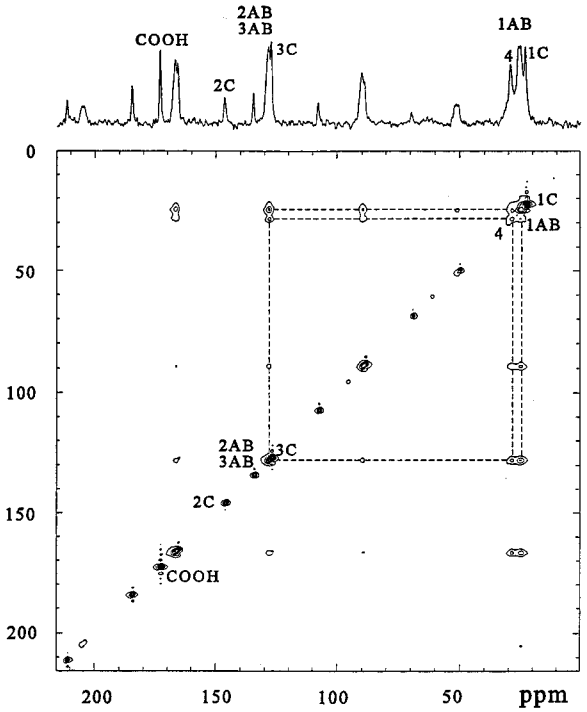

Figure 7. As in Figure 4 for bullvalene carboxylic acid at 30 °C with $\nu_R = 2.9$ kHz and $\tau_m = 20$ ms. One hundred t_1 increments of 50 μs were taken with eight phase-cycled scans per point. Recycle time 5 min, amounting to a total recording time of 2.8 days. Thirty equidistant contours are plotted.

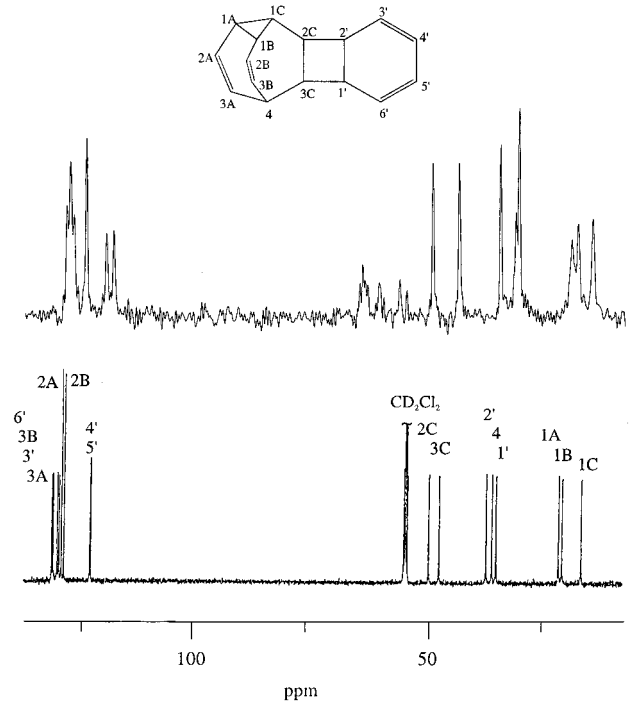

Figure 8. Bottom: Carbon-13 NMR spectra of a solution of the COT dimer in CD_2Cl_2 at −73 °C, with the indicated peak assignment. Top: Carbon-13 CPMAS spectrum of solid COT dimer recorded at 22 °C with $\nu_R = 4.63$ kHz (recycle time 10 min, 10 scans).

It is instructive to compare the kinetic parameters for the rate constants of this process, k_{33}^1, in compounds I and II with those found for k_{13} in solution, since both involve (as a first step) a transition from isomer 3 to isomer 1. For cyanobullvalene E_a of k_{13} was found to be 12.5 kcal mol^{-1} and it is likely to be similar for bullvalenecarboxylic acid. In fact the E_a's of all bond shift processes involving the dominant isomers of monosubstituted bullvalene[1] as well as for bullvalene itself[3] fall within the narrow range of 12.5−15.5 kcal mol^{-1}. The activation energies for k_{33}^1 for compounds I and II (14 kcal mol^{-1}) are at most only 1−2 kcal mol^{-1} higher than for k_{13} in solution, while the actual rate at a fixed temperature (cf. results of Table 6 at −33 °C in ref 1) are one to two orders of magnitude slower for k_{33}^1 in the solid than for k_{13} in solution. This suggests that the dominant factor hindering the process in the solid is an entropy effect.

A similar situation obtains for fluorobullvalene. This compound crystallizes as isomer 4, and it was found that it rearranges via isomers 1 and 3 with a rate equation[2] $k_{44}^{13} = 4.6 \times 10^9$ exp-

($-14.5/RT$) corresponding to an activation entropy of $\Delta S^{\ddagger} \sim -16$ eu. This may be compared with the rate equation k_{14} in fluorobullvalene solutions,[1] $k_{14} = 4.4 \times 10^{11} \exp(-11.9/RT)$ which corresponds to $\Delta S^{\ddagger} \sim -7$ eu. Again, as for compounds I and II, the activation energy for the transformation from the ground isomer to the intermediate isomer is slightly higher in the solid, but there is also an entropy effect on the reaction rate. The kinetic solid state effect is, however, much bigger in the latter case.

We recall that in both types of systems, i.e., those compounds that crystallize as isomer 3 (compounds I and II) and that which crystallizes as isomer 4 (fluorobullvalene), bond shift rearrangements may occur which do not lead to atom permutation and are therefore not detected by NMR. For the compounds which crystallize as isomer 3 this rearrangement involves the sequence 3-2-3, while for the solid with the ground-state isomer 4 it is 4-1-4. On the basis of the above discussion it is very likely that these processes occur at high rates but are unfortunately NMR invisible.

It is worth mentioning that although the line broadening in the 1D dynamic spectra contains all the information regarding the mechanism and rate of the rearrangement process, the 2D exchange spectra display the mechanistic pathway of the reaction in a straightforward and much clearer way. The determination of the reaction pathways in monosubstituted bullvalenes is to our knowledge the first time that transient intermediates have been directly identified in the solid state by such experiments.

Acknowledgment. This research was supported by Grant No. 92-00094/3 from the United States−Israel Binational Science Foundation, Jerusalem, Israel, and by the MINERVA Foundation, Munich/Germany. One of us (K.M.) thanks the Fonds der Chemischen Industrie for financial support.

Supporting Information Available: Tables of crystallographic data and refinement parameters, atomic coordinates, isotropic and anisotropic displacement parameters, and bond distances and angles for **1** and **2** (11 pages). See any current masthead page for ordering and Internet access instructions.

JA954006D